

Stratified slopes, numerical and empirical stability analysis

Author 1

- Rémi Sauffisseau, MEng
- School of Computing, Science and Engineering (CSE), University of Salford, Salford, England
- ORCID [0000-0002-8922-323X](https://orcid.org/0000-0002-8922-323X)

Author 2

- Alireza Ahangar Asr, PhD
- School of Computing, Science and Engineering (CSE), University of Salford, Salford, England
- ORCID [0000-0002-8210-7519](https://orcid.org/0000-0002-8210-7519)

R.Sauffisseau@edu.salford.ac.uk

Abstract

Urbanisation means that many natural slopes in and around cities are often subjected to cuts resulting in dramatic changes in the geometry of slope faces mostly by increasing slope angle which could lead to failures with catastrophic consequences. As most natural slopes are of non-homogeneous layered nature, understanding the stability behaviour of such slopes will be of utmost importance. The current practice in analysing slopes of complicated nature, geometrically and materially, is mostly to apply simplifications sacrificing accuracy leading to use of large factors of safety, which could undermine analytical and economic feasibility of projects. In this research limit-equilibrium and finite element methods are used, respectively by OASYS Slope and PLAXIS 2D, to empirically and numerically model and analyse geometrically non-homogeneous stratified slopes with the aim of understanding the effects of non-homogeneity of geometry and materials on stability under various inclination angles of slope face. The analysis included determination of factors of safety as well as a sensitivity analysis looking into the combined effects of contributing parameters.

Keywords:

Computational mechanics; Geotechnical engineering; Slopes - stabilisation

List of notation

<i>LEM</i>	Limit Equilibrium Method
<i>FEM</i>	Finite Element Method
c'	Effective cohesion
φ'	Effective internal friction angle
<i>C</i>	Slope crest
<i>m</i>	Top of the slip circle (LEM analysis)
<i>n</i>	Bottom of the slip circle (LEM analysis)
<i>FoS</i>	Factor of Safety
β	Slope angle
<i>E</i>	Elastic modulus

1 **1. Introduction**

2 Slope failures are a major problem everywhere in the world because of their human, financial
3 and environmental consequences, causing thousands of deaths due to landslides each year
4 (Kawamoto et al., 2000; USGS, 2016). Therefore, engineers must understand how slopes
5 behave but also how their failures can be prevented. With the expansion of cities and growth in
6 infrastructure construction leading to cuts through natural slopes, engineers ought to deal with
7 slope stability scenarios very often (Bromhead Edward, 2015). This could include road works,
8 dam constructions, bridges or development projects in outskirts of metropolitan cities
9 surrounded by highlands. This outlines the importance of ground investigations to acquire soil
10 stratification to perform stability analysis which can become very expensive and lead to an
11 incomplete or more scattered set of borehole data (Sun, Zhao, Shang, & Zhong, 2013).
12 Ground conditions can be variable even for a small-scale study. Other main variables are water
13 and rainfall intensity (Kawamoto et al., 2000; P. Orense, Shimoma, Maeda, & Towhata, 2004)
14 as well as the geometry of the slope and its material properties (Zhou, Deng, & Xu, 2012). In the
15 past researches, little attention was given to the actual arrangement and orientation of the soil
16 layers and the impact this has on the overall stability of a soil slope. In the research, OASYS
17 analysis is based on the Limit Equilibrium Method (LEM) (Smith, 1981) and the method of slices
18 (Bishop, 1955) while PLAXIS 2D is a finite element method (FEM) based software based on the
19 Shear Strength Reduction Technique (Hammouri, Malkawi, & Yamin, 2008).
20 Since its development and with the assumptions that a cylindrical slip surface will occur,
21 Bishop's (1955) method of slices has been widely used. This method worked based on the
22 assumption that the inter-slice forces are horizontal which satisfies the equilibrium of moments
23 but not the forces in the soil mass. In this research the later method of slices with parallel
24 inclined inter-slice forces (Spencer, 1967), which is a modification to the original method of
25 slices suggested by Bishop (1955), was used. The advantages of the modified Bishop method
26 suggested by Spencer was that it could avoid interlocking problems in the slices. This method
27 enables each slice to remain in equilibrium both horizontally and vertically by calculating the
28 inter-slice forces and satisfies equilibrium of both forces and moments.

29 In this research, the Bishop's method of slices with the advanced parallel inclined method for
30 the inter-slices was used utilising OASYS Slope software. The Factor of Safety against failure
31 for the given probable slip surfaces was calculated using (Bishop, 1955):

$$32 \quad FoS = \frac{\Sigma \text{Resisting Forces}}{\Sigma \text{Driving Forces}}$$

33 1.

34

35 So long as the ratio of the Resisting to Driving Forces is greater than 1, failure will not occur. If
36 the ratio reaches 1, the slope fails.

37

38 With the finite element method, slices and therefore interslice forces are not needed in the
39 process of creating the model and the analysis, and the shape of the slip surface could follow
40 the weakest surface in the soil mass based on the analysis conducted considering the
41 implemented constitutive soil model. According to Griffiths (1999), it is known that finite element
42 lets the failure occur progressively on the model and allows monitoring of the displacements
43 until overall shear failure occurs. Finite element does not use slices as mentioned as opposed to
44 the limit equilibrium methods providing less limitations on the location and shape of the failure
45 surface (Griffiths & Lane, 1999).

46 The shear strength reduction technique is a method which reduces the strength parameters ("c"
47 and "phi" in Mohr-Coulomb soil model) until failure occurs. Using the finite element method for
48 geotechnical analysis creates potential advantages over conventional / empirical methods. The
49 FEM satisfies the input boundary conditions, equilibrium of the model, the constitutive model
50 behaviour and compatibility (physical and mathematical – i.e. no gaps or overlapping occurs
51 within the FE model) (Potts, 1999). The shear strength parameters at failure are then used to
52 calculate the factor of safety of the slope – i.e. the ratio of the initial strength parameters to the
53 ones at failure (Fu & Liao, 2010).

54

55 PLAXIS 2D (2016.1) uses the shear strength reduction technique (reducing cohesion c and
56 angle of frictional resistance φ until failure occurs) to assess the slope stability (Wu, Cheng,
57 Liang, & Cao, 2014) when undertaking the "Safety Calculation". The software works on the

58 basis that reducing the shear strength of soil mass in a slope gradually increases the shear
59 strains propagating from the toe upwards leading to general failure of slope (Matsui & San,
60 1992).

61 While PLAXIS 2D Safety Calculation reduces the shear strength parameters until failure occurs,
62 it is up to the user to define how many calculation steps to undertake – i.e. the user must check
63 that failure has or has not fully occurred before reading the final Safety Factor. If the failure has
64 happened, the Factor of Safety calculated last, will be considered as the required output.

65 However, if failure has not yet occurred, the user must specify additional calculation steps to
66 allow for more strain to develop and for the failure to occur (Vermeer, 1993).

67 **2. Model development process**

68 In order to appreciate the effects that stratification has on the stability of slopes before and after
69 being subject to a cut, two models were developed and named Cases 1 and 2 as will be referred
70 to in the rest of this document. Both models were analysed using the Limit Equilibrium and the
71 Finite Element methods before and after the cut.

72 **Case 1:** The geometry follows the one obtained from the case study presented below (Guo & He,
73 2011). In this case, the slope layers are laid approximately horizontal (Figure 1)

74 **Case 2:** Geometry is changed from Case 1 by rotating the orientation of the layers by almost 90
75 degrees leading to a stratified slope made of near vertical layers of geo-materials (Figure 2).

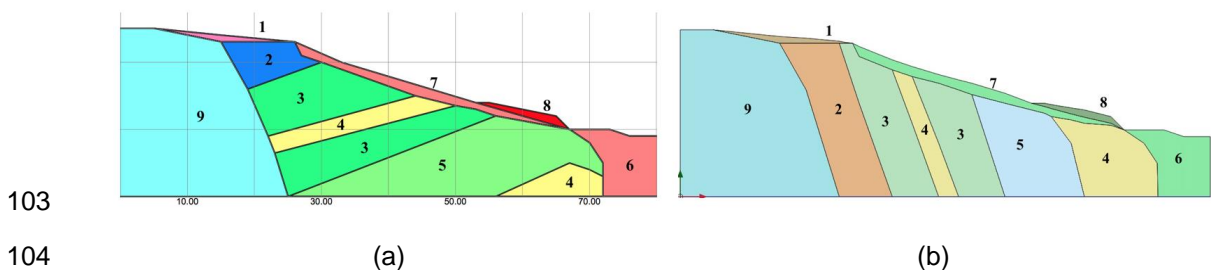
76 Thicknesses of the layers in Cases 1 and 2 were similar as well as the soil type (see Figure 1 and
77 Table 1). The slope face angle (β) in both Cases were 18° before cut (Figure 1) and 56° after cut
78 (Figure 2). The aim of the geometrical modifications made to Case 1 was to observe the effects of
79 the soil layers orientation on the general stability of a stratified slope before and after cut using
80 both limit equilibrium and finite element analysis methods by adopting the Mohr-Coulomb criteria
81 as the governing constitutive model.

82 In all cases studied in this work water table levels were assumed to be sufficiently below the failure
83 surface for the pore water pressure not to be included in the analyses. However, if water table
84 levels were high enough to be included in the model area then the global water table levels and
85 appropriate pore pressure boundary conditions must have been included and activated in the
86 PLAXIS model in appropriate analysis stages according to the site conditions and Terzaghi's

87 principle of effective stress (effective stress = total stress - pore water pressure) would be
 88 implemented for the safety analysis. The models were created and analysed using the Limit
 89 Equilibrium method (LEM) with OASYS Slope and the Finite Element Method (FEM) with PLAXIS
 90 2D software.

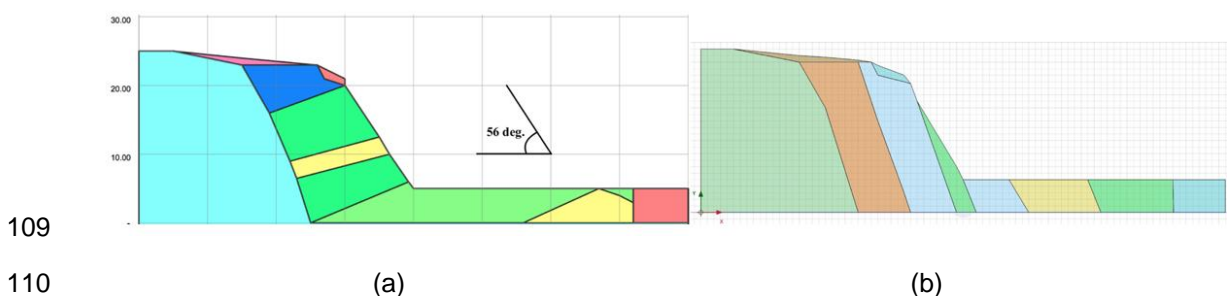
91 The Limit Equilibrium method uses user-defined grids to be used as centre point for the
 92 hypothetical circular slip surfaces to be developed and analysed to locate the slip surface on
 93 which the factor of safety of the slope is the lowest (the most probable slip surface) (Xiao, Yan, &
 94 Cheng, 2011). The Bishop analysis method (Bishop, 1955) was used in these Cases to find the
 95 Factor of Safety on the shear strength in the OASYS analysis using LEM.

96 The Finite Element Method was used using the phi-c reduction technique by PLAXIS 2D software.
 97 In this method the shear strength of the soil mass is reduced in as the analysis progresses in a
 98 step-by-step basis until failure occurs and the calculations are repeated until the stability factor of
 99 safety for the slope is obtained. 15-node triangular isoparametric elements were used in the
 100 analysis and the meshing criteria was set to “very fine” to achieve higher accuracy (Brinkgreve et
 101 al., 2011) in the outputs. Two phases were defined for the analysis with the Initial Stress
 102 Conditions phase being followed by the Factor of Safety calculations.

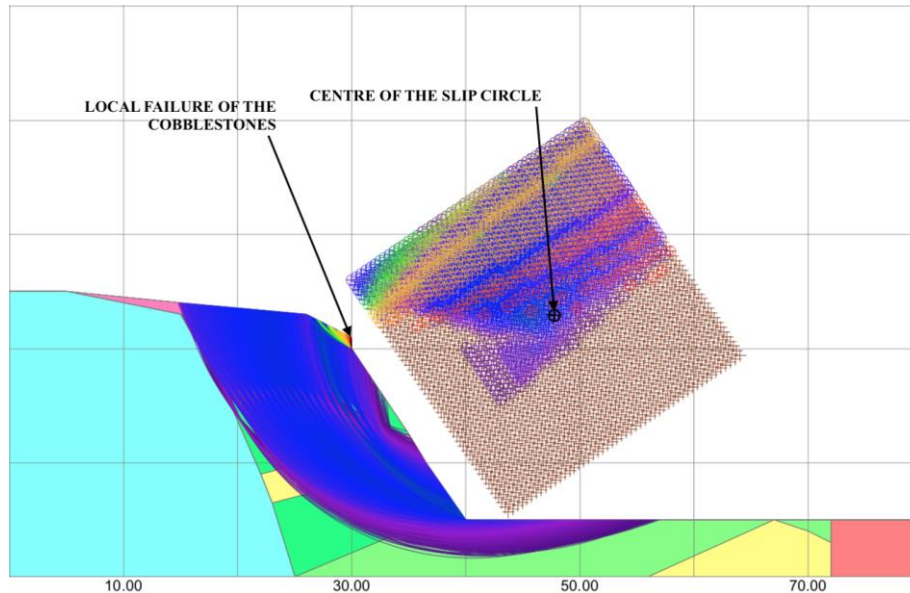


105 Figure 1. Presentation of the models: (a) Case 1 (original); (b) Case 2 (amended layer
 106 orientations) (Numbering corresponds material properties as presented in Table 1)

107
 108



111 Figure 2. Models representing post-cut geometries: (a) Case 1 (b) Case 2 (amended layer
112 orientations)
113 Figure 2 shows the slope after-cut conditions. It must be noted that drained safety analysis was
114 conducted in this research (no water involved in the models) so the excavation was created in
115 one instantaneous step. The first model created (Figure 2a) had a relatively thin layer of
116 cobblestone at the top (Layer 7 in Figure 1) which was replaced later in the analysis by a fill
117 material (soil number 6 in Table 1) due to leading the analysis towards very unusually localised
118 failure of the cobblestones and a very low factor of safety (nearly 0) calculated by the LEM
119 which was out of the scope of this study (Figure 3). Changing the Cobblestone layer to fill
120 material was only done after ensuring that the thickness and positioning of the cobblestone
121 layer was responsible for the very low overall factor of safety for the slope by conducting a trial
122 analysis completed by assuming higher hypothetical shear strength properties for the
123 cobblestone layer (c' and ϕ') which led to the overall output factor of safety of 1.8 for the slope.
124 The cobblestone layer replacement by fill material enabled the study of the overall stability
125 behaviour of the slope.



126
127 Figure 3. Case 1 after cutting - local failure (the small part of Cobblestones is collapsed) issue at
128 the crest due to presence of loose material (cobblestone layer) (OASYS slope model).
129
130 Table 1. Slope material properties used in the LEM and FEM analyses (Guo & He, 2011)

Soil Type	Elastic Modulus (MPa)	Poisson's ratio	Unit Weight (kN/m ³)	Cohesion (kPa)	Friction angle (°)
Filling Soil (6)*	15.1	0.3	18.1	18	20.3
Brown Coal (4)	23.1	0.27	23	16	12
Carbonaceous Mudstone (5)	16.3	0.28	22.5	30	23.2
Mudstone (3)	12.7	0.29	21.2	16.9	16.6
Ophitic (9)	200	0.21	26.2	200	28.35
Dirty Sandstone (2)	120	0.22	27.3	100	33
Soil (1)	80.6	0.26	19.3	18	10.2
Cobble-stones (7)	2000	0.21	21.5	0	24
Clay (8)	40	0.29	19.4	18.3	16

131 *Numbers inside brackets represent material ID numbers as presented in Figure 1 and Figure

132 15.

133

134 3. Model analysis results

135 3.1. OASYS model - LEM analysis

136 3.1.1. Case 1

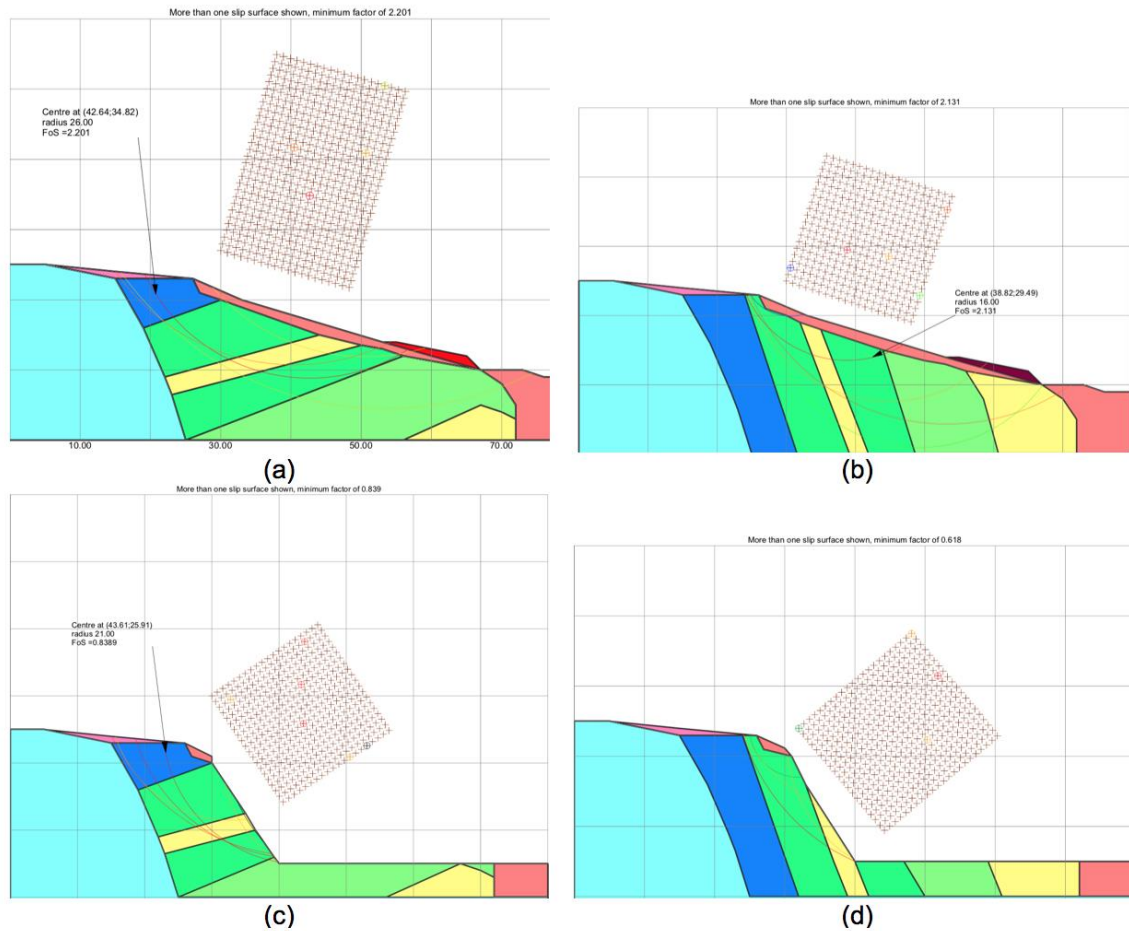
137 The slope was modelled to observe its stability and failure mechanisms prior and following a
138 cut. In its natural environment, the slope (Case 1 shown in Figure 1a) had a factor of safety of
139 2.2 (Figure 4a), which was observed to drop significantly after the removal of the slope material
140 after the cut down to 0.8 (Figure 4c). On the most probable slip surface before the cut (Figure
141 4a), the high point 'm' (x=19m,y=23m; Figure 4a) was located 7m away from the crest of the
142 slope to the left, and the lower point of the slip surface 'n' (x=67m,y=13m; Figure 4a) is placed
143 above the toe of the slope. After the cut (Figure 4c), point 'm' (x=22m,y=23m; Figure 4c) of the
144 slip surface was placed at a point 6m to the left of point C (closer to the crest compared to pre-
145 cut conditions Figure 4a) and reaches the very bottom of the slope where slope and horizontal
146 ground meet (point 'n', in after-cut conditions; x=40m,y=5m; Figure 4c) suggesting that the
147 whole slope will slip down.

148

149 Before the cut, the slip surface goes as deep as 10m, but recovers to a shallower location after
150 the cut getting to the depth of 6m (Figure 4a and 4c).

151 3.1.2. Case 2

152 Prior to any excavation, the stratified slope had a factor of safety of 2.1 (Figure 4b) suggesting
153 that the slope was stable, however the value dropped to 0.6 (unstable slope) after the removal
154 of the slope material (Figure 4d). In the case of the most probable slip surface before the cut,
155 the high point 'm' was located 2m away from the crest 'C' to the left ($x=24m, y=23m$; Figure 4b)
156 and point 'n' (lower point) was located half way down the slope ($x=47m, y=16m$; Figure 4b).
157 Following the cut (Figure 4d), the most probable slip surface at the top starting point (m;
158 $x=24m, y=22m$; Figure 4d) followed the interface of the dirty sandstone and mudstone layers
159 (similar to the pre-cut scenario) and similar to the after-cut conditions in Case 1 (Figure 4c), the
160 slip surface reached the bottom of the slope at the bottom (n; $x=40m, y=5m$; Figure 4d). The
161 failure plane in the case of vertically stratified soil slope was shallower compared to horizontal
162 stratification and the deepest point was recorded at the depth of 5m below the slope surface
163 (Figure 4b).
164
165 Before the cut, the slip surface is located at 5m below the surface (at the deepest part) as well
166 as after the cut (Figure 4b and d). The difference in depth for the slip surface between Case 1
167 and Case 2 post-cut (Figure 4c and d) is not significant compared to the two Cases in pre-cut
168 conditions (Figure 4a and b).



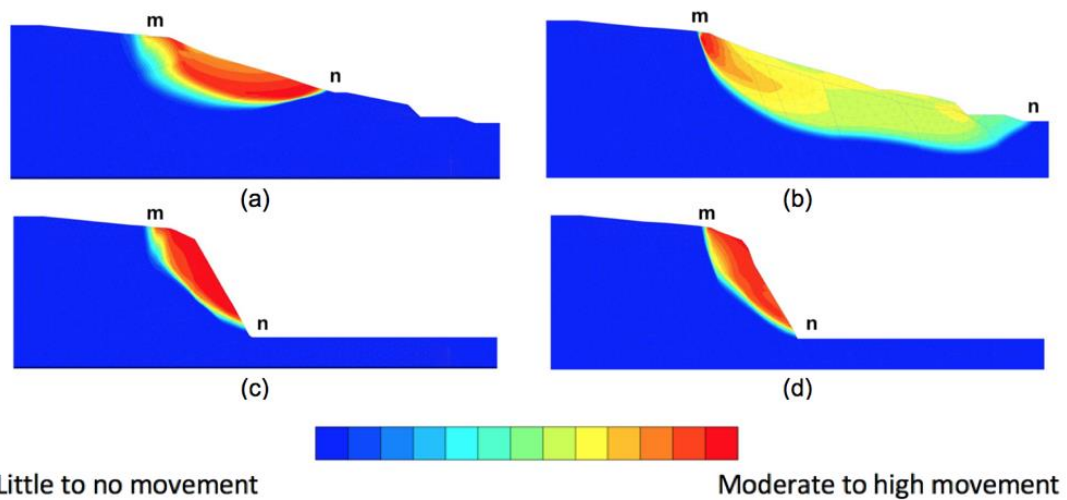
169

170 Figure 4. OASYS Slope LEM; (a) Case 1 Pre-cut, (b) Case 2 Pre-cut, (c) Case 1 post cut and
 171 (d) Case 2 post cut. (Each Distance between consecutive gridlines represents 10m)

172

173 3.2. PLAXIS model FEM analysis

174 Very fine mesh choice for all slope models simulated and analysed using the FEM contributed
 175 to the accuracy of the results. FE results do not rely on a given circular slip surface and give a
 176 more realistic non-circular (when it is the case) slip surface as the slope behaviour affects every
 177 node and elements and the effects they have on each other.



178

179 Figure 5. PLAXIS 2D (FEM analysis): (a) Case 1 Pre-cut; (b) Case 2 Pre-cut; (c) Case 2 post-
 180 cut; (d) Case 2 post-cut.

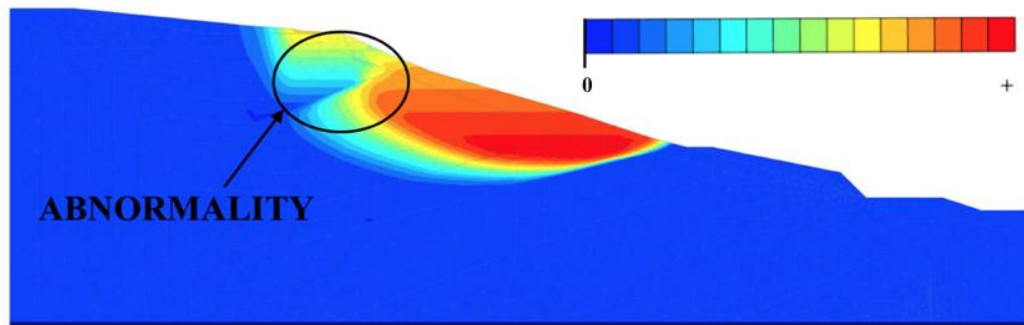
181 For the finite element models created by PLAXIS 2D, a “very fine” mesh was assigned and the
 182 numbers of elements / nodes for the cases before and after excavation were 1097 / 9027 and
 183 766 / 6377 respectively.

184 The FE analysis resulted in different outcomes compared to the LEM. Different factors of safety,
 185 slope failure locations and as well as different shapes of the failure surface were obtained. In
 186 Case 1 (Figure 1a), the factor of safety was 1.8 (stable slope) before the cut but the value
 187 dropped to 0.5 after the cut (Figure 5a and 5c). These values are lower than the values obtained
 188 using the LEM analysis (Figure 4a and 4c).

189 Additionally, in the case of the FEM before the cut (Figure 5a), analysis an abnormality was
 190 observed on the mostly circular slip surface at the location where the dirty sandstone was
 191 placed (Figure 1a) and the slip surface depth was even shallower (Figure 5a). This be explained
 192 by the shear strength parameter values of the material at that point ($c=100$ kPa; $\phi=30^\circ$) which
 193 is considerably higher than the average soil strength parameters as observed in Table 1. The
 194 higher shear strength parameter values interrupted the circular slip surface by creating a dent
 195 and nearly dividing the slip surface to two sections. The effect of this was also reflected in the
 196 factor of safety values where the value changed from 2.2 (LEM) to 1.8 (FEM) (other parameters
 197 based on the methods themselves also affect the changes). This abnormality can also be
 198 observed in the displacements measured in the x (horizontal) and y (vertical) directions.

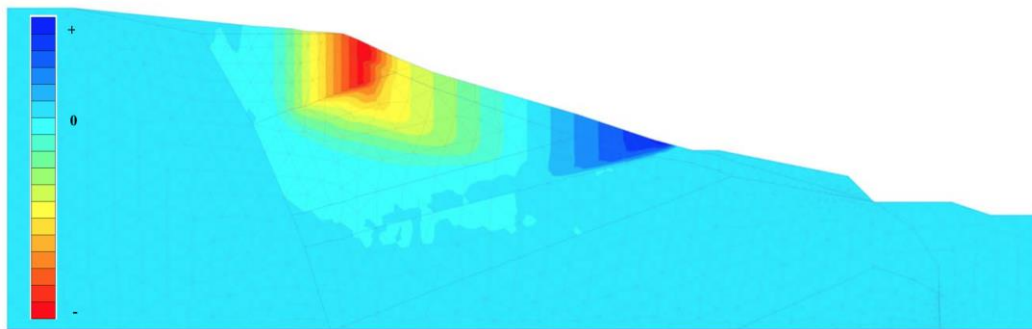
199

200 In Figures 6, 7, 9-14, there are no values for positive and negative maxima represented by the
201 ends of the coloured scales (+/-). Plus sign (+) reflects left-to-right or upwards movements whilst
202 minus sign (-) shows right-to-left or downwards movements. Extreme strain values occur closer
203 the maxima (+ and -).



204

205 Figure 6. Case 1 before cut - displacement in the horizontal direction, (Plus sign shows
206 displacements happening in the left-to-right direction).



207

208 Figure 7. Case 1 before cut y-direction displacement, (Plus sign shows displacements
209 happening in the upwards direction).

210

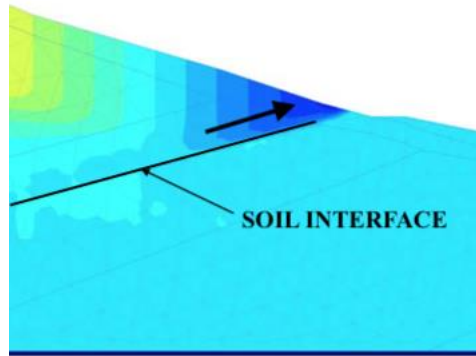
211 As it can be seen in Figure 6 and Figure 7 when the lowest factor of safety was achieved, the
212 top of the most probable slip surface moved downwards while the rest of the slope tended to
213 move in the horizontal direction to the right. This behaviour was expected as was observed
214 before by Jiang and Murakami (2012). It can also be seen from Figure 7 that at the lower
215 boundary of the moving soil mass (blue shaded area in Figure 7), located at the interface
216 between two layers, only the layer on top was subjected to the upward displacement which was
217 induced by the left-to-right sliding of the soil mass on the inclined interface of the Mudstone over
218 the Carbonaceous Mudstone as illustrated in Figure 8.

219

220 Before the cut, the slip surface is located at 6m below the surface (at the deepest point);

221 however, this depth becomes greater after cut and reaches to 9m (Figure 5a and 5c).

222

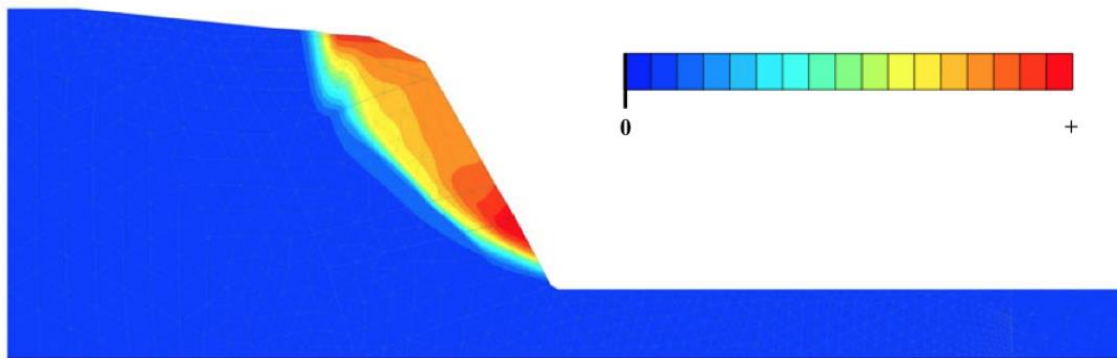


223

224 Figure 8. Inclined displacement of the Brown Coal strata upon the Mudstone strata due to
225 sliding on sloping surface (Figure 1a and Figure 7).

226

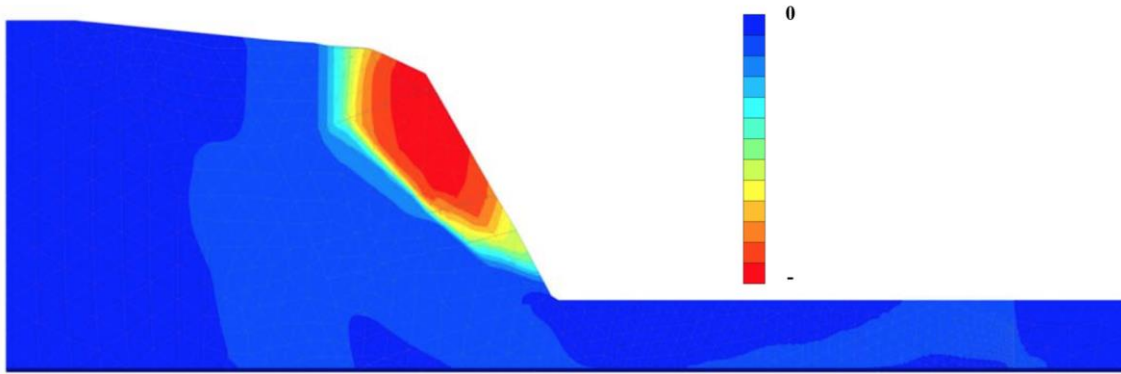
227 After the cut (Figure 5c) and compared to the LEM analysis, it was observed that in the FEM
228 analysis the bottom end of the slip surface (point "n"; $x=39m$ $y=8m$, Figure 5c) was not located
229 at the toe of the slope but at approximately 3m above the toe. Displacements also were
230 obtained in both horizontal (x) and vertical (y) directions (Figure 9 and Figure 10).



231

232 Figure 9. Case 1 - after cut x-direction displacement (Plus sign shows displacements happening
233 in the left-to-right direction).

234

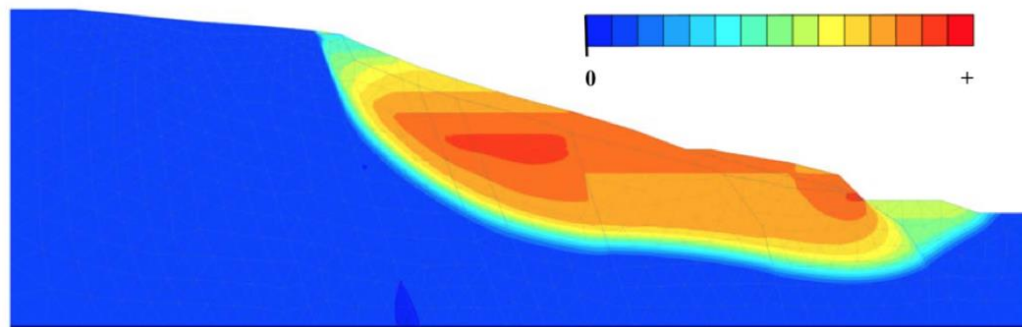


235

236 Figure 10. Case 1 after cut y-direction displacement (Minus sign shows displacements
 237 happening in the downwards direction).

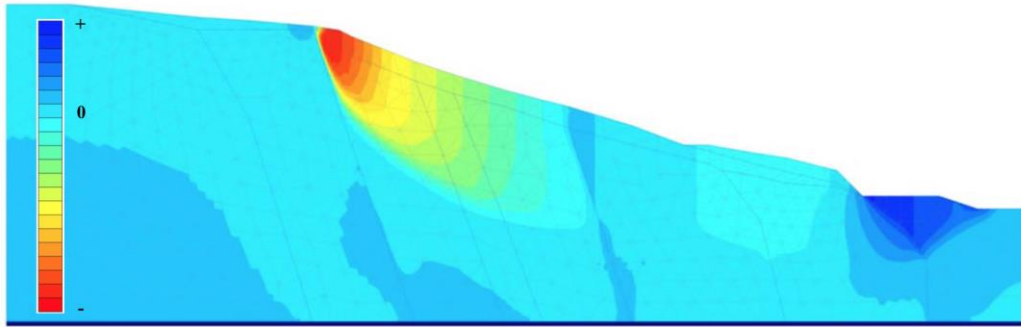
238

239 In case 2, a factor of safety of 2.0 (stable slope - however lower value compared to the LEM
 240 analysis Figure 4b) was obtained before the slope was cut (Figure 5b). Compared to Case 1,
 241 the top of the most probable slip surface (m) was located 2m to the left of point C (same as LEM
 242 analysis results for Case 2 – see Figure 15c) but the bottom end of the slip surface was located
 243 at the very bottom of the slope (n, $x=77m$, $y=8m$). After the removal of the materials during the
 244 cutting process, the factor of safety was calculated to be 0.5 (unstable slope) - Figure 5d; this is
 245 a lower value compared the LEM analysis results -see Figure 4d).



246

247 Figure 11. Case 2 before cut x-direction displacement (Plus sign shows displacements
 248 happening in the left-to-right direction).

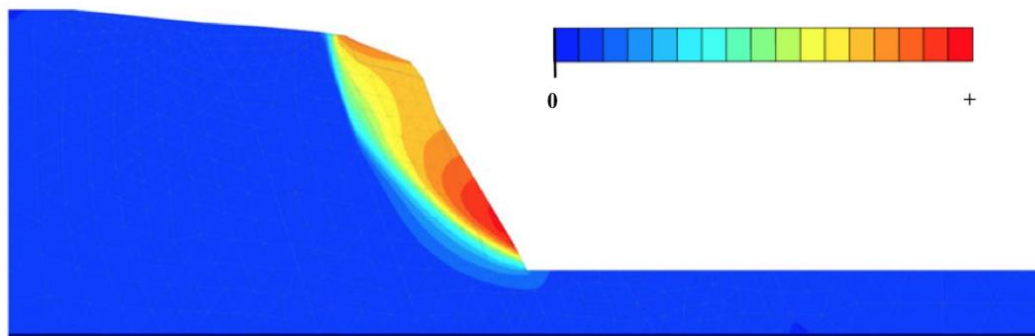


249

250 Figure 12. Case 2 before cut y-direction displacement (Plus sign shows displacements
251 happening in the upwards direction).

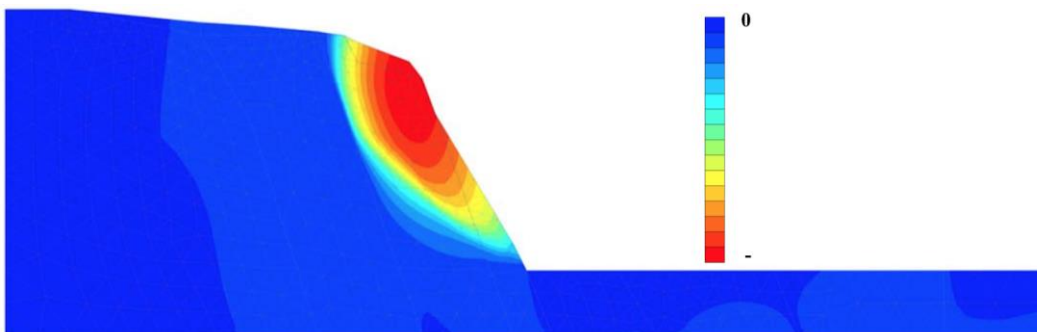
252

253 Before the cut in Case 2, most of the slip surface analysed using the FE method moves
254 horizontally to the right side of the slope (Figure 11) and only the very top left part of the slope
255 surface, as shown in Figure 12, has a significant downward movement along the interface of
256 Dirty Sandstone layer and the Mudstone layer (Figure 1b). Also, as presented in Figure 12, the
257 toe of the slope displays some upwards movement (toe heave) due to the horizontal push
258 observed in the Brown Coal over the Filling Soil (Figure 1b) part of the slope as can be seen in
259 Figure 12.



260

261 Figure 13. Case 2 after cut x-direction displacement (Plus sign shows displacements happening
262 in the left-to-right direction).



263

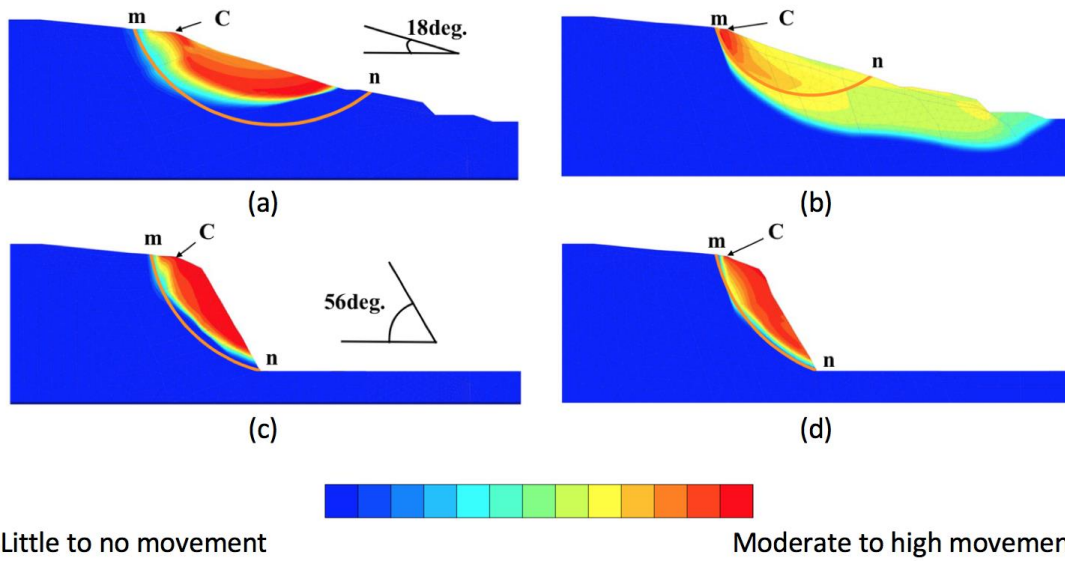
264 Figure 14. Case 2 after cut y-direction displacement (Minus sign shows displacements
265 happening in the downwards direction).
266
267 After the cut in Case 2, while the bottom of the failing mass slides to the right as shown in
268 Figure 13, all the soil mass located on the upper section of the collapsing body falls with a
269 downward movement (Figure 14). As observed in Case 2 with LEM analysis as well, the most
270 probable slip surface falls even more dramatically in the interface of the dirty sandstone and
271 mudstone layers (Figure 5d). This phenomenon more strongly signifies the impact the verticality
272 of the layers on the location of the slip surface and consequently on the values of the factor of
273 safety. Factor of safety from FEM for this surface was 0.5 compared to 0.6 from LEM analysis
274 further emphasizing the effect of orientation of layers. The top of the slip surface (point "m") in
275 the case of FEM analysis of Case 2 had the same location as in the LEM analysis whereas the
276 bottom end, point "n" (x=39m, y=7m), was located 2m above the toe. This presents the same
277 difference as between LEM and FEM analysis for Case 1 as shown above (Figure 5c).
278 Before the cut, the slip surface goes as deep as 10m (at the deepest point) but then recovers to
279 a shallower location after the cut at 6m (Figure 5a and c). It can be observed here that in both
280 cases, the depth at which the slip surface locate itself is more variable depending on the case
281 and even with the two post-cut scenarios with one at 10m (Figure 5c) and the other at 6m
282 (Figure 5d).

283

284 **3.3. Results comparison**

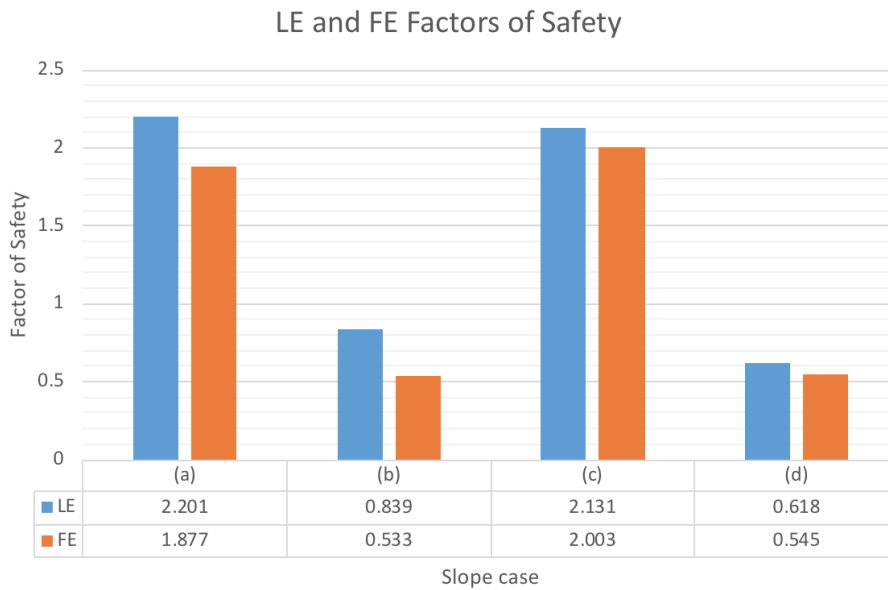
285 In order to observe the differences between LEM and FEM analyses, the results were
286 superimposed and presented in Figure 15.

287



288

289 Figure 15. LEM (bold curves) and FEM analysis results (contours), (a) Case 1 before cutting the
 290 slope; (b) Case 2 before cutting the slope; (c) Case 1 after slope cut; (d) Case 2 after slope cut



291

292 Figure 16. Combined Factor of Safety results for LE and FE: (a) Case 1 before cutting the slope;
 293 (b) Case 1 after slope cut; (c) Case 2 before cutting the slope; (d) Case 2 after slope cut.

294

295 Factors of safety obtained from the LEM analysis were higher compared to the ones obtained
 296 from the finite element method in all cases.

297

298 As a general observation of the results and as expected, the factors of safety from both cases 1
 299 and 2 before the cut were higher compared to the values obtained from the models simulating
 300 after-cut situations. As shown in Figure 16, the factors of safety after the cut were at least 50%
 301 smaller compared to the values relating to before-cut. This might be due to the fact that after a
 302 cut in slope, the slope angle (β) increases dramatically resulting in sharp falls in the stability
 303 factors of safety. Comparing LEM and FEM analysis results reveal that drop in the factor of
 304 safety values is consistent considering both methods; however, values obtained post-cut from
 305 the FEM analysis are much lower (especially in Case 1) compared to the LEM results (Figure
 306 16b). This outcome suggests that implementing the finite element analysis will provide factor of
 307 safety values that will result in safer designs. Indeed, if only LEM analysis was used to calculate
 308 the factor of safety against failure, based on the findings in this research, failure could be
 309 underestimated. This is because obtained value for the factor of safety from FEM analysis (if
 310 conducted) would be smaller making the FEM analysis not only the more accurate but also the
 311 more conservative approach.

312

313 Table 2. Depth of the most probable slip surface for each Case (as illustrated in Figure 1) using
 314 LEM and FEM (depth defined as the length of a hypothetical line perpendicular to the slope
 315 surface connecting the slope surface to the most probable slip surface)

Cases (Figure 1)	LEM	FEM
a	10m	6m
b	5m	10m
c	6m	9m
d	5m	6m

316

317 Table 2 compiles the data for the depth at which the slip surface is located in both cases (Figure
 318 1), pre- and post-cut using both LEM (Figure 4) and FEM (Figure 5).

319 **3.4. Layers material strength effect**

320 Before the cut, the bottom of the slip surface in Case 1 was located at the interface of two layers
 321 at a given depth. The same phenomenon was observed after the cut in Case 2 where a part of
 322 the slip surface followed the vertical interface of two layers. In a vertically stratified slope, the
 323 slip surface depths through each layer is changing. These variations are due to the differences

324 in the shear strength parameters of slope materials in different layers (the higher the shear
325 strength - c' and φ' values, the shallower the slip surface).

326

327 After the cut, the circular pattern generated by the LEM shown in Figure 4c and Figure 4d was
328 similar in both Cases 1 and 2. Important details can also be observed from the FEM analysis.
329 Arrangement of the layers had some effects on the factor of safety and the shear failure in
330 vertically stratified slopes which followed a circular pattern (Figure 15d) as opposed to the linear
331 pattern seen in the horizontally stratified layers case in FEM analysis (Figure 15c).

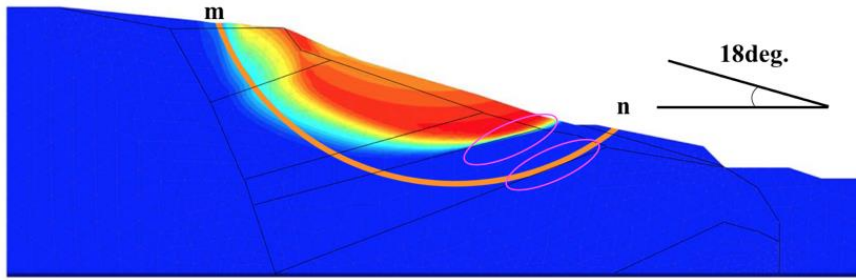
332

333 As observed in the finite element results section, the relative shear strength of different slope
334 materials involved in the analysis and present on the most probable slip surface or in its closest
335 vicinity affects the slip surface location greatly. This shows how a high strength soil (e.g. the
336 dirty sandstone in the examples used in this research - Figure 1a) can have the ability to
337 improve the overall stability factor of safety. Lower layers of soils with higher shear strength
338 contribute significantly towards the relocation of the most probable slip surface to a much
339 shallower position in the slope mass leading also to a smaller failure mass (Figure 5a and
340 Figure 6). This outcome highlights the effect of shear strength of slope material on the actual
341 shape of the failure surface which is not taken into consideration in convention methods of
342 slices due to pre-assumptions made on the shape of the slip surface.

343

344 **3.5. Layers interface effects**

345 Although failure generally happens in the weakest soil, in these cases (i) the slip surface tends
346 to be located at the interfaces rather than within the soil media itself (especially in the case of
347 analysis using the LEM) – i.e. in the cases where the slip surface is at the interface of the
348 Mudstone with the Carbonaceous Mudstone layers (Figure 4a and also pointed at in Figure 17),
349 and (ii) with the FEM, the slip surface linearly followed the interface lines of the two layers - i.e.
350 in the case where the vertically downwards soil mass movement is restrained between the Dirty
351 Sandstone and Mudstone (Figure 5b).



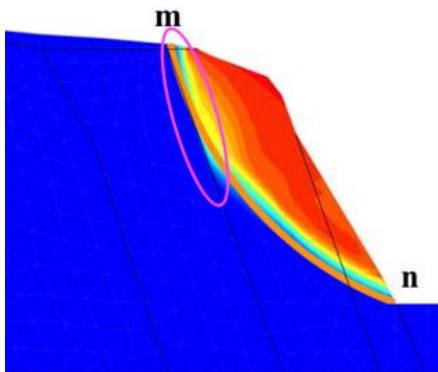
352

353 Figure 17. Case 1 before cut – showing slip surface - layer interface interaction. The soils
 354 interface where slip occurs is encircled; orange curve corresponds to LE result; colour shading
 355 corresponds to FE result (see legend in Figure 15).

356

357 The two encircled zones in Figure 17 show the location of the most probable slip surface in
 358 relation to the layer interface and how they interact. The soil mass involved in the failure
 359 (moving soil mass) restrained by the layer interface the results from LEM and FEM suggest that
 360 if the slope failure is to occur, it is very likely to happen at the interface of two different soils
 361 (Figure 15a,b and d).

362 Observation (ii) can be obtained from the encircled zones - FEM analysis of the probable
 363 circular failure slope surfaces (Figure 17); however, a better example for this observation will
 364 probably be from Case 2 after-cut conditions (Figure 18).



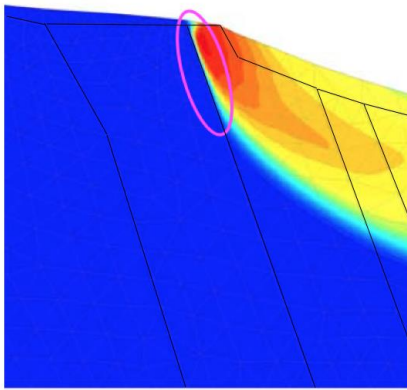
365

366 Figure 18. Case 2 after cut slip/interface interaction. The soil interface where slip occurs is
 367 encircled; bold curve corresponds to LE result; shading/contour corresponds to FE result (see
 368 legend in Figure 15).

369

370 Two observations can be made from Figure 18 concerning the effects of layers in the location of
 371 the slip surface (case 2):

- 372 • In LEM analysis, the beginning of the most probable slip surface (point 'm' in Figure
373 18) is located at the beginning of the vertical interface line between soil layers 2 and
374 3 (Figure 1b and Figure 4b).
 - 375 • In FEM analysis, not only the starting point of the slip is located at the interface of
376 the layers, but the slip surface continues to follow the interface line with depth until
377 the failure surface reaches the point at which it joins the slope toe (Figure 18).
- 378 The second observation from the FEM (mentioned above) is also valid about Case 2 before-cut
379 conditions where at the similar location as for the post-cut (Figure 18) a linear slip surface can
380 be seen (Figure 19).



381
382 Figure 19. Case 2 before cut slip/interface interaction. The soils interface where slip occurs
383 where encircled; shading/contour corresponds to FE result (see legend in Figure 15).
384
385 It is clear in Case 2 before-cut conditions (Figure 19) that the location of the slip surface is
386 constrained by the presence of a layer interface. The encircled area in Figure 19 points out the
387 linear portion of the slip surface from FEM analysis results and the slip surface follows the
388 interface for 6.5m (Figure 19) before starting to curve to join the bottom of the slope (point "n" in
389 Figure 5b), proving the impact the interfaces have on the restriction of the location of the slip
390 surface.

391

392 **3.6. Combined observations from LEM and FEM analysis of Case 1 and Case 2**

393 Before the cut: (i) the bottom of the most probable slip surface in Case 1 (horizontally stratified
394 layers) was located at the interface of two layers (Figure 4a and Figure 5a), (ii) whereas in a
395 vertically stratified slope (Case 2), the slip surface depth in each layer depended on the

396 respective and also relative shear strength of the materials involved in the layers (the higher c'
397 and ϕ' in each soil layer respectively, the shallower the location of the slip surface). The first
398 case (i) was observed in the analysis for the after-cut conditions in Case 2 where a part of the
399 slip surface followed the vertical interface of the two adjacent layers in the vicinity of the slip
400 surface and the second (ii) was observed in Case 2 before the cut where the slip surface depth
401 is changing along depending on the respective layers' shear strength. After the cut in both
402 cases using FEM, arrangement of layers affected the factor of safety and the shear failure in
403 vertically stratified slopes followed a circular pattern (Figure 15d) as opposed to a more linear
404 pattern in the horizontally stratified slope case (Figure 15c). It can be stated that based on the
405 findings of this study, when a stratified slope problem is modelled before construction,
406 simplifications regarding the stratification should be avoided as much as possible. No matter if
407 LEM or FEM analysis is implemented, detailed modelling must be considered to obtain a more
408 realistic understanding of the stability conditions of the slope in terms of the factor of safety as
409 well as the failure pattern of the slope. Indeed, if any stratified slope (most natural slopes) was
410 simplified into a homogeneous slope (even if adequately accurate properties for the equivalent
411 slope material are implemented into the analysis), the impact that the layer orientation and
412 interface would have on the stability will be inevitably ignored leading to inaccurate results
413 especially regarding the failure geometry of the slope and the locations of the most probable slip
414 surface which can significantly affect the design and lead to possible slope failures.

415

416 **4. Conclusions**

417 Limit Equilibrium and Finite Element Methods were used to analyse the stability of horizontally
418 and vertically stratified slopes with the aim of assessing their factor of safety and location and
419 shape of the most probable failure slip surface. Based on the analyses results it can be
420 concluded that in the cases studied in this paper, horizontally stratified slopes (in the settings
421 that implemented in the case studies used to conduct this research) were safer and the analysis
422 resulted in higher factor of safety values in comparison to vertically stratified slopes. However,
423 this outcome cannot be fully generalised to all geometrically non-homogeneous stratified slope
424 cases. Considering similar input and geometry parameter values the Finite Element method
425 could provide more realistic results in terms of the slip surface shape and factor of safety values

426 compared to conventional slope stability analysis methods as it eliminates some simplifications
427 and predetermined failure shape assumptions. The accuracy could further improve by using
428 finer mesh settings. Based on the study outcomes FEM analysis has led to lower factor of safety
429 values compared to the Limit Equilibrium method; however, LEM offers a simpler and quicker
430 way of assessing stability of slope. This makes the use of the finite element method safer for
431 design of structures or excavations in stratified slopes. In addition, outcomes that are more
432 accurate increase the certainty levels leading to lowered design factors of safety (although
433 guidance in Eurocode 7 must be followed) and finally resulting in more economically feasible
434 design. This research focuses on global failures; however, attention must be paid to local
435 failures when using the FE Methods as these may not be always of high concern for global
436 analysis however, they could be misleading and could easily be misinterpreted as global factors
437 of safety.

438 Based on the cases studied in this research, while undertaking a stability analysis of stratified
439 slopes, simplifications regarding the stratification (using an equivalent layer of material with
440 equivalent strength and mechanical properties) must be avoided as much as possible to obtain
441 more realistic representation of the behaviour of slopes; otherwise, whilst the factor of safety
442 values against failure obtained from the analysis could be reasonably close to the reality, the
443 real geometry of the failure of the most probable slip surface could be significantly affected
444 meaning that horizontal or vertical stratification of the slope material layers could lead to
445 completely different failure shapes which could impact the design work and also the
446 construction costs involved depending on the case conditions being considered. However, if the
447 adjacent layers have strength properties with very small differences the simplification by
448 considering equivalent layers could be used with acceptable levels of accuracy. In cases where
449 two layers are significantly different in terms of strength properties this could immensely affect
450 the failure mechanism and the slip surface shape as well as the factor of safety and equivalent
451 layer simplification can be significantly unrealistic.

452 The following conclusions can also be drawn from this study:

- 453 • This research shows that the slope stratification orientation influences the stability, as
454 the factor of safety of a slope in the vertically stratified geo-material was shown to be
455 significantly lower compared to the factor of safety value for the horizontally stratified

456 slope (with similar material layer combination as well as mechanical and strength
 457 properties).

- 458 • The cases studied in this research demonstrated that the layer interface planes are in
 459 cases the most vulnerable locations where part or all of the most probable slip surface
 460 could pass through due to the relative differences between shear strength parameters
 461 in the layers adjacent to the interface plane / slip surface. However, based on the
 462 equilibrium, different cases with different layer arrangements and soil strength and
 463 geometric properties may behave differently.
- 464 • If similar input and geometry parameters were used, based on the outcomes of this
 465 research, the finite element method could provide more realistic results in terms of the
 466 slip surface shapes and the factor of safety values compared to conventional slope
 467 stability analysis methods. This could be due to elimination of some simplifications
 468 including predetermined failure shape assumptions in the finite element method. The
 469 LEM analysis results obtained in this paper were also limited to circular failures.
- 470 • The LEM provides comparably reasonable results and in spite of lacking in accuracy
 471 levels slightly compared to the FEM, this method could be much simpler to use in
 472 analysing slopes. This could be considered a significant advantage provided that the
 473 method is implemented using a reasonably easy to use software with the capability of
 474 taking the effect of stratification into account

476 REFERENCES

- 477
- 478 Bishop, A. W. (1955). The use of the Slip Circle in the Stability Analysis of Slopes.
 479 *Geotechnique*, 5(1), 7-17.
- 480 Brinkgreve, R., Kumarswamy, S., Swolfs, W., Waterman, D., Chesaru, A., Bonnier, P., &
 481 Haxaire, A. (2011). Plaxis 2D Scientific Manual. *I R*.
- 482 Bromhead Edward, N. (2015). ICE manual of geotechnical engineering.
- 483 Fu, W., & Liao, Y. (2010). Non-linear shear strength reduction technique in slope stability
 484 calculation. *Computers and Geotechnics*, 37(3), 288-298.
 485 doi:10.1016/j.compgeo.2009.11.002
- 486 Griffiths, D., & Lane, P. (1999). Slope stability analysis by finite elements. *Geotechnique*, 49(3),
 487 387-403.
- 488 Guo, T., & He, Z. (2011). Comparison of factor of safety of a roadway slope based on the limit
 489 equilibrium method and shear strength reduction method. *Slope Stability and Earth*
 490 *Retaining Walls*, 34-40.

491 Hammouri, N. A., Malkawi, A. I. H., & Yamin, M. M. (2008). Stability analysis of slopes using the
492 finite element method and limiting equilibrium approach. *Bulletin of Engineering*
493 *Geology and the Environment*, 67(4), 471-478.

494 Jiang, M., & Murakami, A. (2012). Distinct element method analyses of idealized bonded-
495 granulate cut slope. *Granular Matter*, 14(3), 393-410.

496 Kawamoto, K., Oda, M., & Suzuki, K. (2000). Hydro- Geological Study of Landslides Caused by
497 Heavy Rainfall on August 1998 in Fukushima, Japan. *Journal of Natural Disaster*
498 *Science*, 22(1), 13-23. doi:10.2328/jnds.22.13

499 Matsui, T., & San, K.-C. (1992). Finite element slope stability analysis by shear strength
500 reduction technique. *SOILS AND FOUNDATIONS*, 32(1), 59-70.
501 doi:10.3208/sandf1972.32.59

502 P. Orense, R., Shimoma, S., Maeda, K., & Towhata, I. (2004). Instrumented Model Slope
503 Failure due to Water Seepage. *Journal of Natural Disaster Science*, 26(1), 15-26.
504 doi:10.2328/jnds.26.15

505 Potts, D. M. (1999). *Finite element analysis in geotechnical engineering: Theory*. London:
506 Thomas Telford Publishing.

507 Smith, M. J. (1981). Soil mechanics. In (4th ed. ed.). London: London : Godwin.

508 Spencer, E. (1967). A method of analysis of the stability of embankments assuming parallel
509 inter-slice forces. *Geotechnique*, 17(1), 11-26.

510 Sun, H.-y., Zhao, Y., Shang, Y.-q., & Zhong, J. (2013). Field measurement and failure forecast
511 during the remediation of a failed cut slope. *Environmental earth sciences*, 69(7), 2179-
512 2187.

513 USGS. (2016). How many deaths result from landslides?

514 Vermeer, P. (1993). PLAXIS 2D reference manual version 5. *Balkema, Rotterdam/Brookfield*,
515 70.

516 Wu, J.-j., Cheng, Q.-g., Liang, X., & Cao, J.-L. (2014). Stability analysis of a high loess slope
517 reinforced by the combination system of soil nails and stabilization piles. *Selected*
518 *Publications from Chinese Universities*, 8(3), 252-259. doi:10.1007/s11709-014-0260-z

519 Xiao, S., Yan, L., & Cheng, Z. (2011). A method combining numerical analysis and limit
520 equilibrium theory to determine potential slip surfaces in soil slopes. *Journal of*
521 *Mountain Science*, 8(5), 718-727. doi:10.1007/s11629-011-2070-2

522 Zhou, J., Deng, J., & Xu, F. (2012). A slope stability analysis method combined with limit
523 equilibrium and finite element simulation. In *Advances in future computer and control*
524 *systems* (pp. 241-247): Springer.

525

526